Subscriber access provided by American Chemical Society

Article

An Investigation on the Analytical Potential of Polymerized Liposomes Bound to Lanthanide Ions for Protein Analysis

Marina Santos, Bidhan C. Roy, Hctor Goicoechea, Andres D. Campiglia, and Sanku Mallik

J. Am. Chem. Soc., **2004**, 126 (34), 10738-10745• DOI: 10.1021/ja048963b • Publication Date (Web): 05 August 2004

Downloaded from http://pubs.acs.org on April 1, 2009

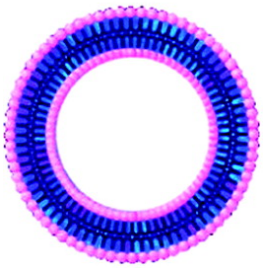

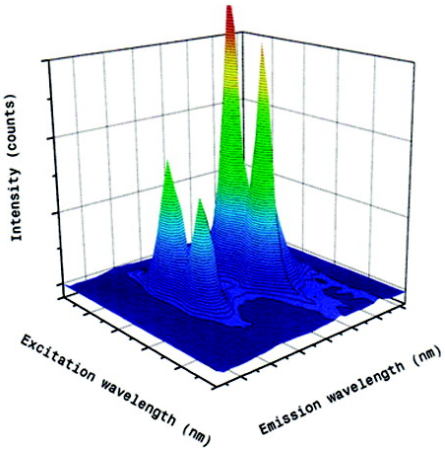

More About This Article

Additional resources and features associated with this article are available within the HTML version:

- Supporting Information
- Links to the 5 articles that cite this article, as of the time of this article download
- Access to high resolution figures
- Links to articles and content related to this article
- Copyright permission to reproduce figures and/or text from this article

View the Full Text HTML

ACS Publications
High quality. High impact.

Journal of the American Chemical Society is published by the American Chemical Society. 1155 Sixteenth Street N.W., Washington, DC 20036

J|A|C|S
ARTICLES
Published on Web 08/05/2004

An Investigation on the Analytical Potential of Polymerized Liposomes Bound to Lanthanide Ions for Protein Analysis

Marina Santos,[†] Bidhan C. Roy,[‡] Héctor Goicoechea,[‡,§] Andres D. Campiglia,*[,†] and Sanku Mallik[‡]

Contribution from the Department of Chemistry, P.O. Box 25000, University of Central Florida, Orlando, Florida 32816-2366, and Department of Chemistry and Molecular Biology, North Dakota State University, Fargo, North Dakota 58105

Received February 24, 2004; E-mail: acampigl@mail.ucf.edu

Abstract: We present a promising approach to protein sensing based on Eu^{3+} ions incorporated into polymerized liposomes. The sensitization of Eu^{3+} is accomplished with 5-aminosalicylic acid, which provides energy transfer for a stable reference signal and a wide wavelength excitation range free from protein interference. The lipophilic character of polymerized liposomes provides the appropriate platform for protein interaction with the lanthanide ion. Quantitative analysis is based on the linear relationship between the luminescence signal of Eu^{3+} and protein concentration. Because no spectral shift of the lanthanide luminescence is observed upon protein interaction, qualitative analysis is based on the luminescence lifetime of polymerized liposomes. This parameter, which changes significantly upon protein−liposome interaction, follows a well-behaved single-exponential decay that might be useful for protein identification.

Introduction

Development of sensing schemes capable of recognizing specific proteins in complex biological matrixes remains an analytical challenge.[1−3] Since 1922, when Wu proposed the use of the Folin phenol reagent to determinate protein concentration,[4] traditional approaches estimate total protein content relying on proteins binding to organic dyes with strong absorption in the ultraviolet and visible regions of the spectrum. The wide scope and good reproducibility of the Lowry protein assay[5] have made it the method generally applied for this purpose. Because of its speed of analysis and sensitivity, the binding assay reported by Bradford[6] has also become a popular alternative among researchers. Despite its popularity, the Bradford procedure presents significant disadvantages. These include different binding stoichiometry between the dye (Coomassie brilliant blue G-250) and different proteins,[7,8] nonlinearity of color yield versus total protein content,[9] and incorrect quantitation of denaturated protein aggregates.[10] Attempts have been made to correct the main disadvantage of the Bradford assay, i.e., the considerable underestimation of protein content of membrane-containing fractions, which rely on sample pretreatment with membrane-disrupting agents such as NaOH[11] or detergents (Triton X-100).[12] These approaches, however, do not address an inherent limitation of the assay, which is the measurement of absorption in the ultraviolet (UV) and visible (vis) ranges of the spectrum. Spectroscopic measurements in the UV−vis are prone to strong matrix interference. Absorption and fluorescence from concomitants can certainly deteriorate limits of detection, reproducibility, and accuracy of analysis.

Recent trends provide higher sensitivity by using fluorescent dyes optically active in the near-infrared, a wavelength region with relatively lower spectral interference from biological matrixes.[13,14] Another sensitive approach is based on the luminescence of lanthanide ions, particularly Eu^{3+} and Tb^{3+}. Their long-lived luminescence is a good match to time-resolved techniques, which discriminate against short-lived background fluorescence and scattered excitation light. Because their emission involves one of the shielded f-level electrons, their luminescence is less sensitive to oxygen quenching than traditional fluorescent dyes.[15−17]

[†] University of Central Florida.
[‡] North Dakota State University.
[§] Current address: Cátedra de Química Analítica I, Facultad de Bioquímica y Ciencias Biológicas, Universidad Nacional del Litoral, Ciudad Universitaria, CC 242-S3000, Santa Fe, Argentina.

(1) Kodadek, T. *Trends Biochem. Sci.* **2002**, *27*, 295.
(2) Kukar, T.; Eckenorde, S.; Gu, Y.; Lian, W.; Meggison, M.; She, J. X.; Wu, D. *Anal. Biochem.* **2002**, *306*, 50.
(3) Lin, H.; Cornish, V. W. *Angew. Chem., Intl. Ed.* **2002**, *41*, 4401.
(4) Wu, H. *J. Biol. Chem.* **1922,** *51*, 33.
(5) Lowry, O. H.; Rosebrough, N. J.; Farr, A. L.; Randal, R. J. *J. Biol. Chem.* **1951,** *193*, 265.
(6) Bradford, M. M. *Anal. Biochem.* **1976**, *72*, 248.
(7) Tal, M.; Silberstain, A.; Nusser, E. *J. Biol. Chem.* **1985**, *250*, 9976.
(8) Kirazov, L. P.; Venkov, L. G.; Kirazov, E. P. *Anal. Biochem.* **1993**, *208*, 44.
(9) Splittgerber, A. G.; Sohl, J. *Anal. Biochem.* **1989**, *179*, 198.
(10) Gotham, S. M.; Fryer, P. J.; Peterson, W. R. *Anal. Biochem.* **1988**, *173*, 353.
(11) Simpson, I. A.; Sonne, O. *Anal. Biochem.* **1982**, *119*, 424.
(12) Gogstad, G. O.; Krutness, M.-B. *Anal. Biochem.* **1982**, *126*, 355.
(13) Lassiter, S. J.; Stryjewski, W.; Owens, C. V.; Flanagan, J. H.; Hammer, R. P.; Khan, S.; Soper, S. A. *Electrophoresis* **2002**, *23*, 1480.
(14) Zhu, L.; Stryjewiski, W.; Lassiter, S.; Soper, S. A. *Anal. Chem.* **2003**, *75*, 2280.
(15) Barbieri, R.; Bertini, I.; Cavallaro, G.; Lee, Y. M.; Luchinat, C. Rosato, A. *J. Am. Chem. Soc.* **2002**, *124*, 5581.

10.1021/ja048963b CCC: $27.50 **© 2004 American Chemical Society**

Offsetting these advantages is the fact that lanthanide's luminescence is quite weak as a result of low molar extinction coefficients, particularly in aqueous solvents. Water molecules strongly bind to the lanthanide ion and quench its luminescence via weak vibronic coupling with the vibrational states of the O−H oscillators.[18] Significant enhancements for analytical use are often achieved with chelating agents that remove water molecules from the lanthanide's primary coordination sphere. The presence of a chelating agent also provides ample opportunity for covalent attachment of a "sensitizer" (or "antenna") to the coordination sphere of the lanthanide ion. Sensitizers are typically organic molecules that strongly absorb and transfer excitation energy to the metal ion, thereby overcoming the inherently weak absorption of lanthanide ions.[19] Because the luminescence lifetimes of lanthanide complexes remain in the microsecond to millisecond time domain, time-discrimination of fluorescence background is still possible.

In this article, we introduce a promising approach to protein sensing based on Eu^{3+} ions incorporated into polymerized liposomes. Polymerized liposomes are spherically closed lipid bilayers with aqueous interior that offer an adequate platform for protein interaction.[20] Unlike unpolymerized vesicles, proteins cannot insert into the lipid bilayer of polymerized liposomes. Instead, they interact with the outer lipid layer of the vesicle via metal−ligand[21,22] and receptor−ligand[23,24] interactions. Because polymerized liposomes are appreciably more stable than their nonpolymerized counterparts, they provide more robust platforms for protein sensing. Lanthanide ions incorporated into polymerized liposomes have been used as magnetic resonance contrast agents,[25,26] but their potential for protein determination has not been explored yet. Similarly, protein sensing via polymerized liposomes has been reported, but their sensing ability has been based on the fluorescence properties of organic dyes.[27,28] Our approach takes advantage of time-resolved lanthanide luminescence to provide a sensitive sensing scheme with potential applications in quantitative and qualitative analysis of target proteins.

Results

Optical spectroscopy has been extensively applied to the study of protein structure. Strong protein absorption and fluorescence emission usually occur below 300 and 450 nm, respectively. Spectral bands are fairly broad and typical full-widths at half-maximum may vary from 45 to 65 nm. As previously mentioned, the spectral region between 200 and 450 nm is undesirable for bioanalytical work as the assay may be prone to primary and secondary inner filter effects. Keeping this possibility in mind, we selected 5-aminosalycilic acid (5As) as the sensitizer. 5As provides the luminescence enhancement needed for reproducible Eu^{3+} signal intensity and a wide wavelength excitation range free from matrix interference. Ethylenediaminetetraacetic acid (EDTA) was chosen as the chelating agent because it forms a tightly bound complex with Eu^{3+} (binding constant being reported as ca. 10^{15} at pH 7).[29] This fact ensures the physical integrity of the probe in the presence of potentially competing ions and/or proteins.

Syntheses of the Complexes. Reports on polymerized liposomes capable of complexing lanthanide ions are relatively few. To the extent of our literature search, only one article previous to our work[30,31] reports on a polymerized liposome containing Gd^{3+} for magnetic resonance imaging use.[25,26,32] The syntheses of 5As−EDTA−Eu^{3+} and the polymerizable lipid incorporating this complex as the headgroup (lipid **1**.Eu^{3+}) are shown in Scheme 1. The carboxylic acid group of EDTA−triethyl ester[33] was activated with NHS and DCC; the resultant active ester was combined with 5As to afford the amide-ester **4**. The free acid group of compound **4** was then coupled with the reported polymerizable amine **5**[31] to yield the lipid **1** in protected form. The ester groups were hydrolyzed with LiOH; lowering the pH of the reaction mixture to 3.0 (with HCl) precipitated the lipid as a white solid. Small and giant polymerized liposomes from lipid **1**.Eu^{3+} (10 wt %, 90% polymerizable phosphocholine **PC1**) were prepared following literature procedures.[34−37] The giant liposomes were found to precipitate soon after polymerization; hence, these liposomes were not investigated any further.

Spectral Characteristics of the Polymerized Liposomes. Figure 1A shows the steady state (SS) excitation and emission spectrum of EDTA−Eu^{3+} at neutral pH (25mM HEPES buffer). Luminescence excitation at 395 nm promotes five characteristic bands resulting from the electronic transitions that occur from the $^5D_0$ to the ^7F manifold. The most intense bands correspond to the $^5D_0-^7F_1$ (593 nm) and $^5D_0-^7F_2$ (616 nm) transitions. The peaks at 580 nm ($^5D_0-^7F_0$), 651 nm ($^5D_0-^7F_3$), and 698 nm ($^5D_0-^7F_4$) result from forbidden transitions and, therefore, are relatively weak. Figure 1B shows the SS excitation and fluorescence spectra of 5As. The maximum excitation at 326 nm reduces the possibility of primary inner filter effects from proteins. Because its fluorescence overlaps with the 466 nm excitation peak of EDTA−Eu^{3+}, the possibility of energy transfer exists.

Figure 2A shows the SS excitation and emission spectra of the complex (5As−EDTA−Eu^{3+}). The broad excitation and emission bands are attributed to the presence of the antenna. The relatively weak luminescence from Eu^{3+} is overwhelmed by the strong fluorescence of 5As, and its contribution to the

(16) Bemquerer, M. P.; Bloch, C.; Brito, H. F.; Teotonio, E. E. S.; Miranda, M. T. M. *J. Inorg. Biochem.* **2002**, *9*, 363.
(17) Franz, K. J.; Nitz, M.; Imperiali, B. *ChemBioChem* **2003**, *4*, 265.
(18) Wu, S. L.; Horrocks, W. D., Jr. *Anal. Chem.* **1996**, *68*, 394.
(19) Sabbatini, N.; Guardigli, M.; Lehn, J.-M *Coord. Chem. Rev.* **1993**, *123*, 201.
(20) Lasic, D. D. *Liposomes: From Physics to Applications*; Elsevier: New York, 1993.
(21) Megli, F. M.; Selvaggi, M.; Huber, R. *Biochemistry* **1998**, *37*, 10540.
(22) Shnek, D. R.; Pack, D. W.; Sasaki, D. Y.; Arnold, F. H. *Langmuir* **1994**, *10*, 2382.
(23) Kitano, H.; Kato, N.; Ise, N. *Biotechnol. Appl. Biochem.* **1991**, *14*, 192.
(24) Kitano, H.; Sohda, K.; Kosaka, A. *Bioconjugate Chem.* **1995**, *6*, 131.
(25) Storrs, R. W.; Tropper, F. D.; Li, H. Y.; Song, C. K.; Kuniyoshi, J. K.; Stipkins, D. A.; Li, K. C. P.; Bednarski, M. D. *J. Am. Chem. Soc.* **1995**, *117*, 7301.
(26) Sipkings, D. A.; Cheresh, D. A.; Kazemi, M. R.; Nevin, L. M.; Bednarsky, M. D. *Nat. Med. (N.Y.)* **1998**, *4*, 623.
(27) Stora, T.; Lakey, J. H.; Vogel, H. *Angew. Chem., Int. Ed.* **1999**, *38*, 389.
(28) Malony, K. M.; Shnek, D. R.; Sasaki, D. Y.; Arnold, F. H. *Chem. Biol.* **1996**, *3*, 185.
(29) Parker, D.; Gareth Williams, J. A. *J. Chem. Soc., Dalton Trans.* **1996**, 3613.
(30) Roy, B. C.; Fazal, M. A.; Arruda, A. F.; Mallik, S.; Campiglia, A. D. *Org. Lett.* **2000**, *2*, 3067.
(31) Roy, B. C.; Santos, M.; Mallik, S.; Campiglia, A. D. *J. Org. Chem.* **2003**, *68*, 3999.
(32) Bednarski, M. D.; Lee, J. W.; Callstorm, M. R.; Li, K. C. P. *Radiology* **1977**, *204*, 263.
(33) Burks, E.; Koshti, N.; Jacobs, H.; Gopalan, A. *Synlett* **1998**, 1285.
(34) Moscho, A.; Orwar, O.; Chiu, D. T.; Modi, B. P.; Zare, R. N. *Proc. Natl. Acad. Sci. U.S.A.* **1996**, *93*, 11443.
(35) Jaeger, D. A.; Zeng, Z. *Langmuir* **2003**, *19*, 8721.
(36) Jaeger, D. A.; Clark, T. C. *Langmuir* **2002**, *18*, 3495.
(37) Akashi, K.; Miyata, H.; Itoh, H.; Kinosita, K., Jr. *Biophys. J.* **1996**, *71*, 3242.

Scheme 1. Syntheses of 5As−EDTA−Eu^{3+} and the Polymerizable Lipid Incorporating This Complex as the Head Group (Lipid **1**.Eu^{3+}) Are Shown[a]

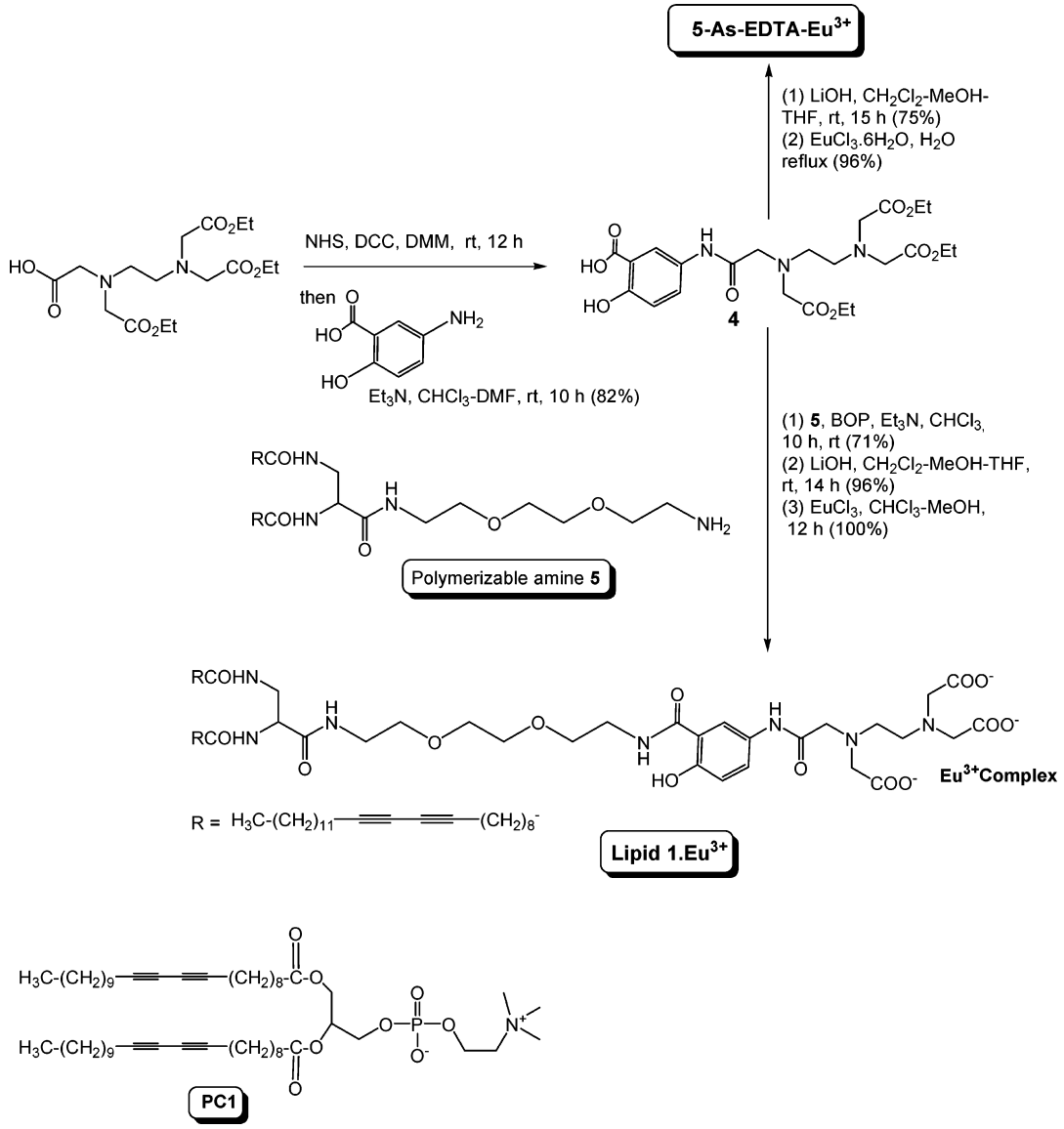

[a] Also shown is the structure of the polymerizable phosphocholine **PC1** used as the major component of the liposomes.

SS spectrum is unnoticeable. Figure 2B depicts the SS excitation and emission spectrum of the complex incorporated into the liposome. Its comparison to Figure 2A shows broader excitation and emission bands and red-shifts in both wavelength maxima. These changes are attributed to the fluorescence contribution from the backbone of the polymerized liposomes. Similar to the unbound complex, the luminescence of Eu^{3+} does not appear in the SS spectrum of the polymerized liposome. It only appears in the time-resolved (TR) spectrum. A 150 μs delay removes the fluorescence contribution from the antenna and the liposomes providing a probe that relies only on the emission wavelengths of Eu^{3+}.

Figure 3A depicts the TR excitation−emission matrix of the polymerized liposomes. Although the strongest excitation occurs between 275 and 325 nm, a wide excitation range is available to promote luminescence from the lanthanide ion. This versatility provides ample opportunity for finding an appropriate excitation wavelength with no matrix interference. Figure 3B compares the luminescence emitted by the lanthanide ion upon excitation at 298 nm, 326 nm (the maximum wavelength of the antenna), and 395 nm, i.e., a wavelength for the direct excitation of Eu^{3+} (see Figure 1A). The best signal-to-noise (S/N) ratio away from protein absorption was clearly obtained via energy transfer from the antenna. This excitation wavelength (326 nm) was then used for all further studies.

Absorption and Fluorescence Characteristics of Target Proteins. Three proteins were randomly selected for our studies, namely, bovine serum albumin, carbonic anhydrase (bovine erythrocyte), and γ-globulin (bovine serum). Table 1 relates their absorption and fluorescence characteristics at neutral pH. As expected, the three proteins show strong absorption and fluorescence within 200−320 nm and 350−450 nm, respectively. Their absorptivities decrease with increasing wavelength and become negligible at the excitation (λ_{exc} = 326 nm) and the emission (λ_{em} = 615 nm) wavelengths of the proposed sensor. Their fluorescence intensities show similar wavelength dependence but, under steady-state conditions, interfere with the reference signal. Because their fluorescence decays are

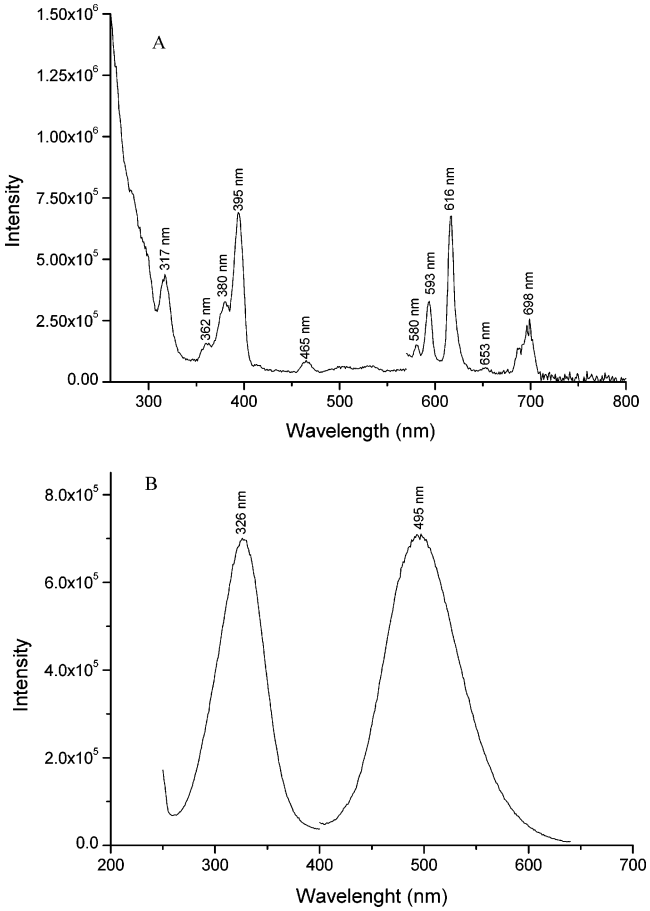

Figure 1. Steady-state excitation and emission spectra recorded from (A) 10^{-3} M Eu−EDTA and (B) 10^{-6} M 5As solutions. Both solutions were prepared in 25 mM HEPES. (A) Spectra were recorded using 10 and 5 nm excitation and emission band-pass, respectively. A cutoff filter was used at 550 nm to avoid second-order emission. (B) Spectra were recorded using 15 and 2 nm excitation and emission band-pass, respectively.

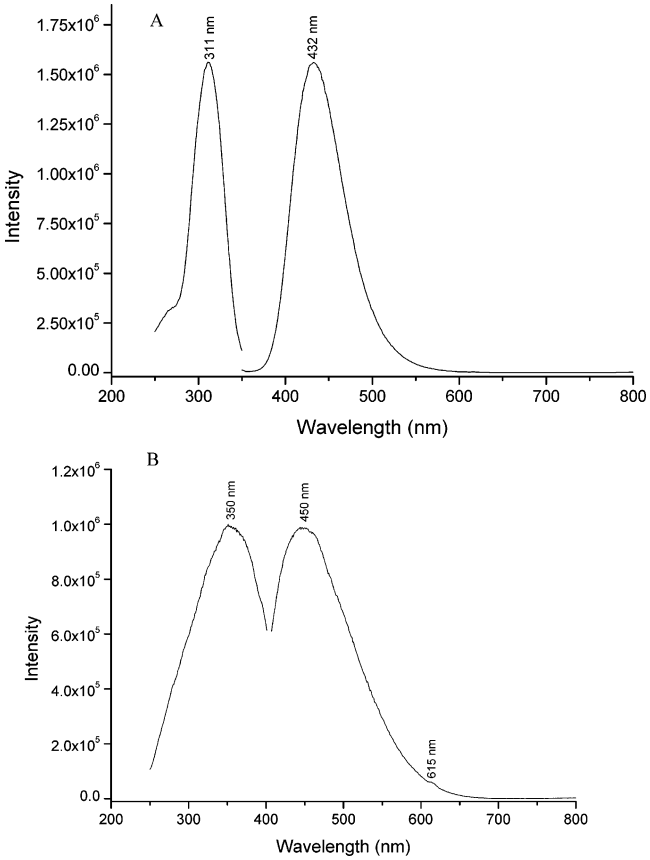

Figure 2. Steady-state excitation and emission spectra recorded from (A) 10^{-3} M 5As−EDTA−Eu^{3+} and (B) 92.3 mg·L^{-1}polymerized liposome solutions. Both solutions were prepared in 25 mM HEPES. (A) Spectra were recorded using 2 nm excitation and emission band-pass. (B) Spectra were recorded using 7 and 2 nm excitation and emission band-pass, respectively.

shorter than the fluorescence decay of the polymerized liposomes, using a 150 μs delay also eliminates protein fluorescence interference. In fact, under these instrumental parameters, there is no protein contribution to either primary or secondary inner filter effects.

Number of Eu^{3+} Sites Available for Protein Interaction. Eu^{3+} can accommodate up to eight or nine molecules of water in its first (inner) coordination sphere.[38] When solvents containing OH groups are coordinated to Eu^{3+}, efficient nonradiative deactivation of the excited $^5D_0$ level takes place via weak vibronic coupling with the vibrational states of the O−H oscillators. Because the O−H oscillators act independently, the overall effect on the rate of radiationless deactivation is proportional to the number of O−H oscillators in the inner coordination sphere of Eu^{3+}. If the O−H oscillators are replaced by the lower frequency O−D oscillators, the vibronic deactivation pathway becomes much less efficient. As a result, the luminescence lifetime of the lanthanide ion is enhanced, and the lifetime of the excited state becomes longer. The differences in the effects of H_2O and D_2O upon luminescence lifetimes can be used to determine the number of water molecules coordinated to Eu^{3+}. The number of water molecules can be determined with the following equation: $q = A_{LN}(\tau_{H2O}^{-1} - \tau_{D2O}^{-1})$,[38] where q is the number of water molecules in the first coordination sphere of Eu^{3+}, A_{LN} is the proportionality constant (1.05) for Eu^{3+}, and τ_{H2O} and τ_{D2O} are the luminescence lifetimes of the liposome in H_2O and D_2O, respectively.

Assuming that protein−liposome interaction would replace water molecules in the inner coordination sphere of Eu^{3+}, we determined the number of available sites for metal−protein interaction as the number of lanthanide-coordinated water molecules. Lifetime experiments were carried out with liposome solutions prepared in aqueous buffer (25 mM HEPES) or in aqueous buffer: D_2O mixtures containing different volume ratios of H_2O−D_2O. All measurements were made at $\lambda_{exc}/\lambda_{em}$ = 326/615 nm. The lifetime in water (τ_{H2O} = 223.0 ± 7 μs) was obtained from the average of six independent measurements directly taken from the polymerized liposomes in aqueous buffer (25 mM HEPES). The D_2O value (τ_{D2O} = 638.8 μs) was obtained from extrapolation of the linear plot between the experimental reciprocal luminescence lifetime (τ^{-1}) and the mole fraction of water (χ_{H2O}) in H_2O−D_2O mixtures (see Figure 4). The number of coordinated water molecules was calculated as 3.06, which is in good agreement with the fact that EDTA was synthesized to coordinate five sites in the first coordination sphere of the lanthanide ion.

Quantitative Analysis with the Polymerized Liposomes. Similar to the expected effect on the luminescence lifetime, the

(38) Horrocks, W. D., Jr.; Sudnick, D. R. *Acc. Chem. Res.* **1981**, *14*, 384.

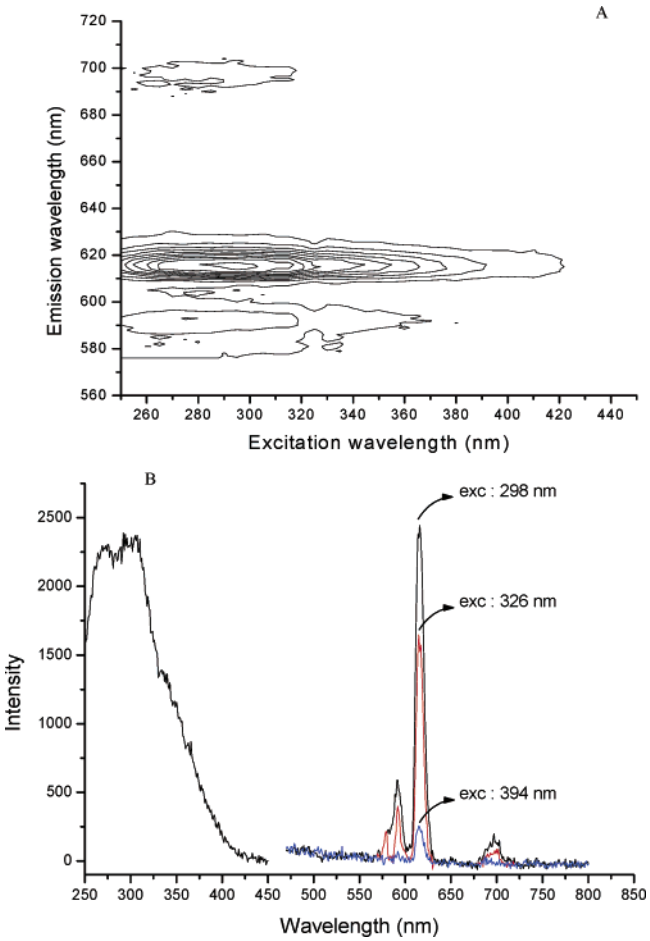

Figure 3. (A) Time-resolved excitation−emission matrix and (B) time-resolved luminescence spectra (500−800 nm) recorded at three excitation wavelengths from a 92.3 mg·L^{-1} polymerized liposome solution prepared in 25 mM HEPES. All spectra were recorded using 30 and 2 nm excitation and emission band-pass, respectively. Other acquisition parameters were 150 μs delay and 1000 μs integration time. A cutoff filter was used at 450 nm to avoid second-order emission. (B) Excitation spectrum (250−450 nm) was recorded monitoring the luminescence intensity at 615 nm.

Table 1. Absorption and Fluorescence Characteristics of Target Proteins

protein[a]	λ_{max}; $a_{\lambda max}$[b] (nm; L·cm^{-1}·g^{-1})	a_{326}; a_{615}[c] (L·cm^{-1}·g^{-1})	λ_{exc}; λ_{em}[d] (nm)	IR[e]
albumin	278; 1.9	0.25; 0.02	269; 342	3.6×10^{-4}
carbonic anhydrase	279; 2.6	0.76; 0.23	282; 340	0.01
γ-globulin	278; 2.4	0.27; 0.01	270; 334	6.6×10^{-4}

[a] Protein solutions (30 mg/L) were prepared in 25 mM HEPES buffer, pH = 7.0. [b] λ_{max} = maximum absorption wavelength; $a_{\lambda max}$ = absorptivity at maximum absorption wavelength. [c] Protein absorptivities at 326 and 615 nm. [d] Maximum excitation (λ_{exc}) and fluorescence (λ_{em}) wavelengths. [e] IR = intensity ratio between fluorescence at 326 and 615 nm and at the maximum excitation and emission wavelengths (λ_{exc}; λ_{em}).

presence of D_2O enhanced the luminescence signal of the polymerized liposomes. The luminescence enhancement was directly proportional to χ_{D2O}. Predicting a similar effect in the presence of the target proteins, we evaluated the quantitative performance of the proposed sensor. Initial studies tested the batch-to-batch reproducibility of the liposome signal. Signal variations within 1 order of magnitude were observed from batch to batch. The lack of reproducibility results from different final concentrations of 5As−EDTA−Eu^{3+} in the liposome.

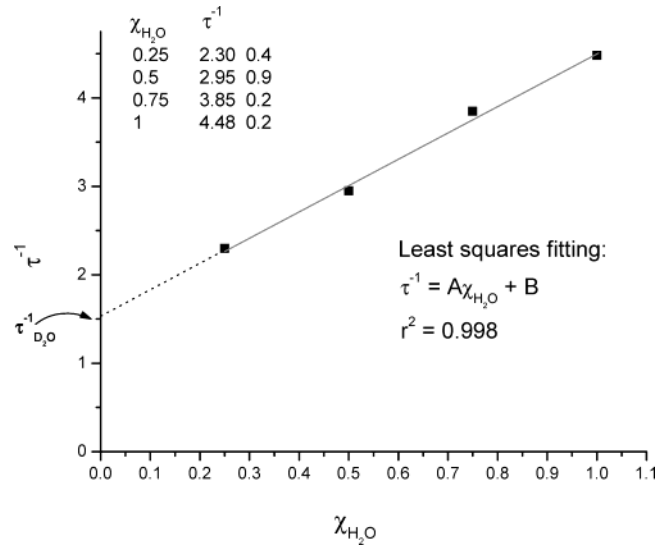

Figure 4. Reciprocal luminescence lifetime (τ^{-1}) in μs^{-1} as a function of mole fraction of water (χ_{H2O}) in D_2O-H_2O mixtures in Eu−EDTA (1:1) solution. $A = 1.535 \pm 0.1017\ \mu s^{-1}$, and $B = \tau_{D2O}^{-1} = 1.565 \times 10^{-3}\ \mu s^{-1}$.

Table 2. Analytical Figures of Merit[a] Obtained with the Liposome Sensor

protein[b]	LDR[c] (mg·L^{-1})	R^2 [d]	γ[e] (mg·L^{-1})	RSD[f] (%)	LOD[g] (mg·L^{-1})
albumin	1.8−27.0	0.9990	15 620	3	1.8
CA	1.7−24.5	0.9992	16 260	3	1.7
γ-globulin	0.90−18.0	0.9991	47 360	2	0.9

[a] Analytical figures of merit were obtained with commercial spectrofluorimeter. [b] Protein solutions were prepared in 25 mM HEPES. CA = carbonic anhydrase. [c] LDR = linear dynamic range of calibration curve defined from the limit of detection to the upper linear concentration. [d] R = variance of calibration curve. [e] γ = analytical sensitivity defined as the slope of the calibration curve divided by the precision of measurements at medium concentration. [f] RSD = relative standard deviations at medium concentrations. [g] LOD = limit of detection. Values correspond to the protein concentration giving a signal $y = y_B + 3s_B$, where y_B is the average signal in the absence of protein and s_B is its standard deviation.

A convenient way to eliminate batch-to-batch variability was to work with appropriate amounts of liposome that provided the same 5As−EDTA−Eu^{3+} concentration in all analytical samples. The final concentration was chosen to be 5×10^{-6} M. At this concentration, the S/N was 20 and the relative standard deviation of sixteen determinations ($N = 16$) was 2.6%. Liposome working solutions were prepared upon appropriate dilutions with HEPES buffer (neutral pH). The dilution factors were based on the complex concentration in the original liposome sample. The original concentration was determined with the method of standard additions. This approach was the method of choice to compensate for potential matrix interference. Different volumes of a concentrated 5As−EDTA−Eu^{3+} solution were added to several different sample aliquots of the same liposome volume. The volumes of the standard additions were negligible in comparison to the liposome volumes to ensure that the sample matrix was not significantly changed by dilution with the added standards. The luminescence signal was monitored in the presence of various protein concentrations, and the measurements were made in batch (25 mH HEPES, neutral pH). To account for signal stabilization, measurements were done after 15 min of protein mixing.

Table 2 summaries the analytical figures of merit obtained for the three proteins. The luminescence intensities plotted in

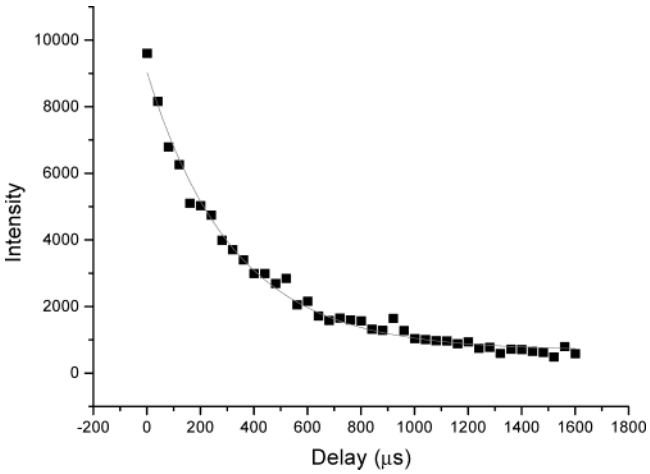

Figure 5. Fitted luminescence decay curve for polymerized liposome in the presence of carbonic anhydrase. Experimental parameters for wavelength−time matrix collection were the following: $\lambda_{exc}/\lambda_{em}$ = 326/615 nm, time delay = 1000 ns, gate width = 500 000 ns, gate step = 40 000 ns, number of accumulations per spectrum = 100 laser pulses, number of kinetic series per wavelength time matrix = 40, and slit-width of spectrograph: 1 mm. Polymerized liposome and carbonic anhydrase were mixed in 25 mM HEPES to produce final concentrations of 92.3 mg·L^{-1} and 24.5 mg·L^{-1}, respectively.

the calibration graphs are the average of individual measurements taken from three aliquots of the same working solution. The linear dynamic ranges of the calibration curves are based on at least five protein concentrations. The correlation coefficients (R) and the slopes of the log−log plots (data not shown) are close in unity, demonstrating a linear relationship between protein concentration and signal intensity. The relative standard deviations, which are based on individual measurements of six aliquots of the same working solution, demonstrate the excellent precision of measurements. The lower limit of detection obtained for γ-globulin is in agreement with the higher sensitivity of the sensor toward this protein.

Qualitative Potential of Polymerized Liposomes. Because no spectral shift is observed in the presence of proteins, extracting qualitative information from the luminescence spectrum of the liposome is not possible. However, the replacement of OH oscillators by the OD variety causes a significant change to the luminescence lifetime of the liposome ($\Delta\tau$ = 415.8 ± 17.9 μs). Assuming a similar effect upon protein binding, and knowing that the luminescence lifetime is usually sensitive to the microenvironment of the luminophor, we investigated the feasibility of using this parameter for qualitative analysis of proteins. The experiments were carried out in batch (25 mM HEPES) with a fixed concentration of liposome (92.3 mg·L^{-1}). The exponential decays were collected at $\lambda_{exc}/\lambda_{em}$ = 326/615 nm after 15 min of protein mixing. Protein concentrations in the final mixtures were at the upper limit concentration of their respective linear dynamic ranges (see Table 2).

Figure 5 shows a typical decay in the presence of carbonic anhydrase. The agreement between the calculated and observed points over the first two lifetimes of the decays agreed to within about 1%, and the residuals showed no systematic trends. Single exponential decays with excellent fittings were also observed for albumin and γ-globulin. These facts suggest that only one type of microenvironment per protein surrounds the lanthanide ion or that only one type of microenvironment significantly contributes to the observed lifetime. Table 3 compares the reference lifetime (absence of protein) to the lifetimes in the presence of the target proteins. For a confidence level of 95% (α = 0.05; $N_1 = N_2$ = 6),[39] the reference value was statistically different to the lifetime in the presence of proteins, demonstrating that the lifetime of the liposomes is sufficiently sensitive to probe the presence of a target protein on the bases of lifetime analysis. The lifetime in the presence of carbonic anhydrase was statistically different (P = 0.05, $N_1 = N_2$ = 6) to the lifetimes in the presence of the other two proteins. It is possible, therefore, to use the liposome sensor to identify carbonic anhydrase against albumin and γ-globulin. On the other end, albumin and γ-globulin provided statistically equivalent (P = 0.05, $N_1 = N_2$ = 6) lifetimes. The inability to differentiate between these two proteins shows the need for an additional parameter to improve the selectivity of the proposed sensor toward a target protein.

Table 3. Comparison of Luminescence Lifetimes Measured with the Liposome Sensor in the Absence and the Presence of Proteins

protein[a]	lifetime[b] (μs)	RSD[c] (%)
−	233.0 ± 7.0	3.1
albumin	294.0 ± 7.6	2.6
γ-globulin	301 ± 8.0	2.6
carbonic anhydrase	353.3 ± 7.5	2.1

[a] Protein solutions were mixed with a fixed concentration of liposome (92.3 mg·L^{-1}) to provide the following final concentrations: 27 mg·L^{-1} of albumin, 24.5 mg·L^{-1} of carbonic anhydrase, and 18.0 mg·L^{-1} of γ-globulin. All solutions were prepared in 25 mM HEPES. [b] Liposome lifetimes are the averages of six measurements taken from six aliquots of sample solution. All measurements were made at $\lambda_{exc}/\lambda_{em}$ = 326/615 nm. [c] RSD = relative standard deviations of luminescence lifetimes.

Discussion

Our studies demonstrate the feasibility of using the luminescence response of 5As−EDTA−Eu^{3+} incorporated into polymerized liposomes to monitor protein concentrations in aqueous media. The energy transfer needed for the sensitization of the lanthanide ion is obtained from the antenna, providing a reproducible reference signal for protein determination at the parts per million level. Quantitative analysis is based on the linear relationship between the luminescence signal of the liposome and protein concentration. The luminescence enhancement is attributed to the removal of water molecules from the coordination sphere of Eu^{3+} upon protein interaction. Although a straightforward comparison with the limits of detection reported in the literature is difficult as different instrumental setups, experimental, and mathematical approaches have been used for their determination,[40−46] our results provide an overall improvement of at least 1 order of magnitude. Qualitative analysis is based on the luminescence lifetime of the liposome. This parameter follows well-behaved single exponential decays in the absence and the presence of proteins. The shortest lifetime

(39) Miller, J. C.; Miller, J. N. *Statistics for Analytical Chemistry*; Wiley: New York, 1984.
(40) Malony, K. M.; Shnek, D. R.; Sasaki, D. Y.; Arnold, F. H. *Chem. Biol.* **1996**, *3*, 185.
(41) Jelinek, R.; Okada, S.; Norvez, S.; Charych, D. *Chem. Biol.* **1998**, *5*, 619.
(42) Hainik, T.; Snejdarkova, M.; Meszar, E.; Krivanek, R.; Tvarozek, V.; Novotny, I.; Wang, J. *Sens. Actuators, B* **1999**, *57*, 201.
(43) Okada, S. Y.; Jelinek, R.; Charych, D. *Angew. Chem., Int. Ed.* **1999**, *38*, 655.
(44) Stora, T.; Lakey, J. H.; Vogel, H. *Angew. Chem., Int. Ed.* **1999**, *38*, 389.
(45) Cheng, Q.; Peng, T.; Stevens, R. C. *J. Am. Chem. Soc.* **1999**, *121*, 6767.
(46) Patolsky, F.; Lichtenstein, A.; Willner, I. *J. Am. Chem. Soc.* **2000**, *122*, 418.

is observed in the absence of proteins, which agrees with our assumption for luminescence enhancement and protein−liposome interaction. Because the lifetime of the liposome changes significantly upon protein interaction, the potential for protein identification on the bases of lifetime analysis exists. However, the fact that two of the target proteins showed statistically equivalent lifetimes demonstrates the need for additional selectivity. Future studies will attempt a selectivity enhancement based on template polymerization. We will create polymerized liposomes with templates complementary to the patterns of target proteins to directly determine them in complex matrixes without previous separation.

Materials and Methods

Reagents. All reagents and solvents were purchased from commercial suppliers and used without further purification. Nanopure water was used throughout. Polymerizable 8,10-heneicosadiynoic acid was used as obtained from GFS Chemicals. Spectroscopy grade organic solvents from Fisher Scientific were used. All aqueous solutions were prepared from Nanopure water (Millipore). Experiments were conducted under an atmosphere of dry nitrogen. For workup, the organic layer was dried on anhydrous Na_2SO_4 and concentrated in vacuo. Elemental analyses were performed by an in-house materials characterization laboratory. TLC was performed with Absorsil Plus 1P, 20 × 20 cm^2 plate, 0.25 μm (Alltech Associates, Inc.). Chromatography plates were visualized either with UV light or in an iodine chamber. ^{1}H, ^{13}C NMR spectra were recorded using 300 and 500 MHz spectrometers in one of the following solvents: $CDCl_3$, D_2O, and CD_3OD with TMS as internal standard. ^{13}C NMR spectra data were reported with two digitals after the decimal to distinguish between close resonance. ^{13}C NMR spectra of lipid **1** could be studied because of the poor solubility in common organic solvents.

Compound 4. EDTA ester (1.10 g, 2.92 mmol) was dissolved in dry ethyl acetate (30 mL), followed by the addition of NHS (0.37 g, 3.22 mmol) and DCC (0.665 g, 3.22 mmol) at room temperature. Stirring was continued at room temperature for another 12 h. The white precipitate was filtered under nitrogen and washed with ice-cold ethyl acetate. Solvent was removed from the filtrate in vacuo. The viscous liquid was again dissolved in dry $CHCl_3$ (25 mL). 5-Amino salicylic acid.HCl (0.470 g, 3.07 mmol) was dissolved in DMF (5 mL) in the presence of Et_3N (0.7 mL, 5.03 mmol) and added dropwise. The reaction mixture was stirred at room temperature for 10 h and quenched with water. The organic layer was washed with water and dried over Na_2SO_4. The crude product was purified by silica gel column chromatography with 15% MeOH in $CHCl_3$ (R_f = 0.2). Yield: 0.67 g (82%, with respect to consumed EDTA−ester: 0.6 g). ^{1}H NMR (500 MHz, $CDCl_3$): δ 1.39 (t, 9H, J = 7.2 Hz), 2.78−2.95 (m, 4H), 3.49 (s, 2H), 3.58 (s, 6H), 4.20 (q, 4H, J = 7.2 Hz), 4.25 (q, 2H, J = 7.2 Hz), 4.34−4.38 (bs, 1H), 6.89 (d, 1H, J = 8.6 Hz), 8.64 (dd, 1H, J = 2.7 and 8.6 Hz), 8.12 (d, 1H, J = 2.7 Hz).

Compound **4** (0.14 g, 0.27 mmol) was dissolved in CH_2Cl_2/THF/MeOH (2/4/2 mL), and solid LiOH (85 mg, 2.02 mmol) was added. The reaction mixture was stirred at room temperature for 15 h. The pH of the solution was adjusted to 3.0 with 6 N HCl. The solvents were removed in vacuo, the residue was again dissolved in minimum-volume MeOH (300 μL), and THF/CH_2Cl_2 (2/2 mL) was added. The white precipitate was filtered off and washed with THF and then dried. Yield: 95 mg (69%). ^{1}H NMR (300 MHz, D_2O): δ 3.29−3.34 (m, 2H), 3.47−3.53 (m, 2H), 3.71 (s, 2H), 3.79 (s, 2H), 3.90 (s, 4H), 6.95 (d, 1H, J = 8.8 Hz), 7.51 (dd, 1H, J = 3.0 and 8.8 Hz), 7.86 (d, 1H, J = 3.0 Hz). Calcd for $C_{17}H_{21}N_3O_{10}$.HCl: C, 43.98; H, 4.74; N, 9.05. Found: C, 43.71; H, 4.53; N, 8.76.

5As−EDTA−Eu^{3+} Complex. The acid from the previous step (41 mg, 0.082 mmol) was dissolved in 5 mL of Nanopure water and solid $EuCl_3 \cdot 6H_2O$ (30 mg, 0.082 mmol) was added. It was refluxed for 4 h and solvent was removed in vacuo to afford the complex as a white solid (54 mg, 96%). Anal. Calcd for $C_{17}H_{18}N_3O_{10} \cdot 4H_2O.2HCl$: C, 28.12; H, 3.86; N, 5.79. Found: C, 27.84; H, 3.64; N, 5.75.

Lipid 1. Polymerizable amine-HCl salt **5**[2] (0.3 g, 0.296 mmol) was dissolved in dry $CHCl_3$ in the presence of Et_3N, followed by the addition of BOP reagent (0.14 g, 0.32 mmol) and compound **4** (0.17 g, 0.33 mmol). The coupling was carried out at room temperature for 10 h. The reaction was quenched with saturated NaCl solution. The organic solvent was removed in vacuo when the product precipitated as a white solid. It was filtered and washed with water. The pure product was obtained by silica gel column chromatography with 8% MeOH in $CHCl_3$ (R_f = 0.4) to afford polymerizable ester. Yield: 0.31 g (71%). ^{1}HNR (300 MHz, $CDCl_3$−CD_3OD): δ 0.91 (t, 6H, J = 7.1 Hz), 1.25−1.42 (m, 53H), 1.52−1.65 (m, 16H), 2.18−2.29 (m, 16H), 3.40−3.47 (m, 8H), 3.52−3.60 (m, 8H), 3.64−3.66 (m, 4H), 3.71 (s, 6H), 4.13−4.25 (m, 6H), 4.48 (bs, 2H), 4.51−4.56 (m, 1H), 6.94 (d, 1H, J = 8.5 Hz), 7.32−7.36 (bs, 1H), 7.56 (dd, 1H, J = 3 and 8.5 Hz), 7.65−7.78 (bs, 1H), 7.77−7.81 (bs, 1H), 8.12 (d, 1H, J = 8.5 Hz). ^{13}C (125 MHz, $CDCl_3$−CD_3OD): δ 14.13, 14.18, 19.22, 22.74, 25.56, 25.63, 25.71, 25.76, 28.42, 28.88, 28.91, 29.02, 29.05, 29.15, 29.28, 29.39, 29.53, 29.65, 29.68, 31.96, 36.39, 39.21, 39.28, 39.32, 39.42, 41.44, 41.62, 52.24, 53.07, 54.03, 54.24, 55.16, 56.30, 59.08, 60.89, 61.08, 65.27, 65.38, 68.23, 69.55, 69.67, 70.23, 70.28, 70.34, 77.42, 68.23, 69.55, 69.67, 70.23, 70.28, 70.34, 77.42, 77.65, 114.69, 118.02, 118.22, 126.17, 129.37, 170.34, 170.42, 171.37, 171.64, 174.74, 174.82, 175.51, 175.53.

The above ester (0.145 g, 0.99 mmol) was dissolved in CH_2Cl_2/THF/MeOH (2/2/4 mL), and solid LiOH (25 mg, 0.99 mmol) was added. The reaction mixture was stirred at room temperature for 14 h. The pH of the solution was adjusted to 3.0 with 1 N HCl. The organic solvents were removed in vacuo, and water was added. The white precipitated solid was filtered, washed with water, and dried in vacuo. Yield: 132 mg (92%).^{1}H NMR (500 MHz, $CDCl_3$−CD_3OD−D_2O): δ 0.92 (t, 6H, J = 7.1 Hz), 1.25−1.35 (m, 42H), 1.38−1.45 (m, 6H), 1.53−1.56 (m, 8H), 1.60−1.64 (m, 4H), 2.19−2.23 (m, 4H), 2.26−2.29 (m, 12H), 3.37−3.44 (, 4H), 3.48−3.54 (m, 10H), 3.57−3.61 (m, 2H), 3.64−3.68 (m, 6H), 3.71−3.74 (m, 4H), 4.52−4.56 (m, 1H), 6.93 (d, 1H, J = 8.6 Hz), 7.71 (m, 1H), 7.90 (d, 1H, J = 8.6 Hz).

Lipid.Eu^{3+} Complex. Lipid **1** (100 mg, 0.072 mmol) was dissolved in CH_3Cl_3/MeOH (3/3 mL), and solid $EuCl_3 \cdot 6H_2O$ (26.4 mg, 0.072 mmol) was added. The reaction mixture was stirred for 24 h at room temperature. The solvents were removed in vacuo, and the white solid was dried. Yield: 110 mg (100%). Anal. Calcd for $C_{76}H_{118}N_3O_{14} \cdot 2H_2O$: C, 59.15; H, 8.04; N, 6.35. Found: C, 59.47; H, 8.44; N, 6.10.

Instrumentation. Excitation and emission spectra were collected with a commercial spectrofluorimeter (Photon Technology International). For steady-state measurements, the excitation source was a continuous-wave 75 W xenon lamp with broadband illumination from 200 to 2000 nm. Detection was made with a photomultiplier tube (PMT, model 1527) with wavelength range from 185 to 650 nm. The method of detection was analogue for high signal levels or photon counting for low signal levels. In analogue mode, the inherent peak-to-peak noise was 50 × 10^{-12} A with 0.05 ms time constant. In photon counting mode, the maximum count rate was 4 MHz, pulse pair resolution 250 ns, rise time 20 ns, and fall time 100 ns with a 220 ns pulse width. For time-resolved measurements, the excitation source was a pulsed 75 W xenon lamp (wavelength range from 200 to 2000 nm), variable repetition rate from 0 to 100 pulses/s, and a pulse width of approximately 3 μs. Detection was by means of a gated analogue PMT (model R928) with extended wavelength range from 185 to 900 nm. SS and TR spectra were collected with excitation and emission monochromators having the same reciprocal linear dispersion (4 nm·mm^{-1}) and accuracy (±1 nm with 0.25 nm resolution). Their 1200 grooves/mm gratings were blazed at 300 and 400 nm, respectively. The instrument was computer controlled using commercial software (Felix32) specifically designed for the system.

Luminescence lifetimes were measured with an instrumental setup mounted in our lab.[47] Samples were excited directing the output of a Northern Lights tunable dye laser (Dakota Technologies, Inc.) through a KDP frequency-doubling crystal. The dye laser was operated on LDS 698 (Exiton), and it was pumped with the second harmonic of a 10 Hz Nd:YAG Q-switched solid-state laser (Big Sky Laser Technologies). Luminescence was detected with a multichannel detector consisting of a front-illuminated intensified charge fiber-coupled device (ICCD, Andor Technology). The minimum gate time (full width at half-maximum) of the intensifier was 2 ns. The CCD had the following specifications: active area = 690 × 256 pixels (26 mm^2 pixel size photocathode), dark current = 0.002 electrons/pixel/s, and readout noise = four electrons at 20 kHz. The ICCD was mounted at the exit focal plane of a spectrograph (SPEX 270M) equipped with a 1200 grooves/mm grating blazed at 500 nm. The system was used in the external trigger mode. The gating parameters (gate delay, gate width, and the gate step) were controlled with a digital delay generator (DG535, Stanford Research Systems, Inc.) via a GPIB interface. Custom LabView software (National Instruments) was developed in-house for complete instrumental control and data collection.

Measurements and Procedures. Measurements with the spectrofluorimeter were made with standard quartz cuvettes (1 cm × 1 cm). A fiber optic probe was used with the laser system. The probe assembly consisted of one excitation and six collection fibers fed into a 1.25 m long section of copper tubing that provided mechanical support. All the fibers were 3 m long and 500 μm core diameter silica-clad silica with polyimide buffer coating (Polymicro Technologies, Inc.). At the analysis end, the excitation and emission fibers were arranged in a conventional six-around-one configuration, bundled with vacuum epoxy (Torr-Seal, Varian) and fed into a metal sleeve for mechanical support. The copper tubing was flared, stopping a swage nut tapped to allow for the threading of a 0.75 mL polypropylene sample vial. At the instrument end, the excitation fiber was positioned in an ST connection and aligned with the beam of the tunable dye laser, while the emission fibers were bundled with vacuum epoxy in a slit configuration, fed into a metal sleeve, and aligned with the entrance slit of the spectrometer.

Luminescence lifetimes were determined via a three-step procedure:[47] (1) collection of full sample and background wavelength−time matrixes, (2) subtraction of background decay curve from the luminescence decay curve at the target wavelengths of the sensor, and (3) fitting the background-corrected data to single exponential decays. The decay curve data were collected with a minimum 150 μs interval between opening of the ICCD gate and the rising edge of the laser pulse, which was sufficient to avoid the need to consider convolution of the laser pulse with the analyte signal (laser pulse width = 5 ns). In addition, the 150 μs delay completely removed the fluorescence of the sample matrix from the measurement. Fitted decay curves $\{y = y_0 + A_1 [-\exp(x - x_0)t_1]\}$ were obtained with Origin software (version 5, Microcal Software, Inc.) by fixing y_0 and x_0 at a value of zero.

Acknowledgment. This research was supported by the National Institute of General Medical Sciences (NIH 1 RO1 GM 63204-01A1 to S.M. and A. C.) and the National Science Foundation (CHE-0138093 to A. C.).

Note Added after ASAP Posting. A spelling error in the abstract was corrected on August 6, 2004.

JA048963B

(47) Bystol, A. J.; Campiglia, A. D.; Gillispie, G. D. *Anal. Chem.* **2001**, *73*, 5762.